Macromolecules

Article

pubs.acs.org/Macromolecules

Hierarchical Structure Analysis of Graft-Type Polymer Electrolyte Membranes Consisting of Cross-Linked Polytetrafluoroethylene by Small-Angle Scattering in a Wide-*Q* Range

Hiroki Iwase,[†,‡,⊥] Shin-ichi Sawada,[†] Tetsuya Yamaki,[†] Satoshi Koizumi,*[,‡,∥] Masato Ohnuma,[§] and Yasunari Maekawa*[,†]

[†]High Performance Polymer Group, Quantum Beam Science Directorate (QuBS), Japan Atomic Energy Agency (JAEA), 1233 Watanuki, Takasaki, Gunma 370-1292, Japan

[‡]Strong Correlated Supramolecular Group, QuBS, JAEA, Tokai, Ibaraki 319-1195, Japan

[§]Quantum Beam Center, National Institute for Materials Science, (NIMS), 1-2-1 Sengen, Tsukuba, Ibaraki 305-0047 Japan

ABSTRACT: Small-angle scattering in a wide-Q range (4×10^{-3} to 1.5 nm^{-1}) of polymer electrolyte membranes consisting of poly(styrenesulfonic acid) and cross-linked polytetrafluoroethylene (cPTFE−PEM) with various grafting degrees up to 36% was observed by focusing small-angle neutron scattering (FSANS), small-angle neutron scattering (SANS), and small-angle X-ray scattering (SAXS). The hierarchical structure of the PEM was characterized as being composed of conducting layers (graft domains) in lamellar stacks with 48−57 nm spacing on the surfaces of 480 nm diameter crystallites and ultrasmall structures with 1.7 nm correlation distance of the sulfonic acid groups in the conducting layers. The PEMs with grafting degrees less than 15% possessed only grafting domains in the amorphous layers of the lamellar stacks of cPTFE. An increase in the grafting degree up to 5% led to an increase in the lamellar spacing of 20%, while the lamellar spacing remained constant with grafting degrees above 5% because of crystalline restriction. Moreover, with grafting degrees of greater than 15%, grafting domains were phase-separated from the cPTFE substrate and covered the crystallites with a diameter of 480 nm (the length of a crystallite is above the observed *Q* region (>1.6 μm). The graft domains around the crystallites were connected with the adjoining domains; accordingly, the PEMs with a higher degree of grafting had conductivity higher than that of Nafion. Furthermore, in the SAXS measurement, the nano-order internal structure (1.7 nm) corresponded to the distance between the sulfonic acid groups of the graft polymers in the conducting layers of the cPTFE−PEM. The nano-order correlation distances of the sulfo groups, which cannot be observed in Nafion, should result in methanol and water crossover levels lower than those in Nafion.

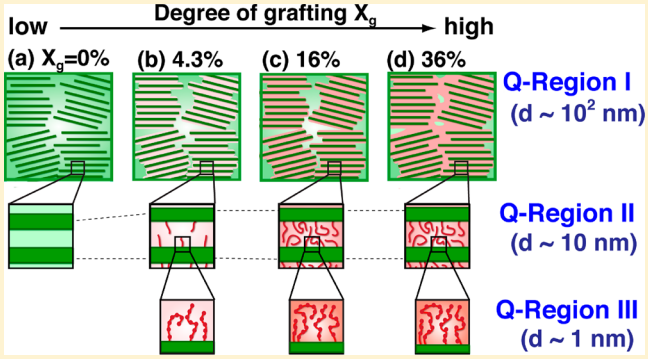

INTRODUCTION

Polymer electrolyte membranes (PEMs) are one of the most important components of polymer electrolyte fuel cells (PEFCs) and direct methanol fuel cells (DMFCs), because the PEM plays an important role in the selective transport of protons from the anode to the cathode while avoiding fuel (H_2 or methanol) crossover. Perfluorinated polymer membranes such as Nafion (DuPont), which consists of a polytetrafluoroethylene (PTFE)-like backbone with side chains containing a sulfonic acid group, have usually been used as a PEM in PEFC and DMFC systems because of its favorable mechanical and chemical stability, along with its higher proton conductivity in the hydrated state.[1] However, perfluorinated PEMs have several limitations for practical use, such as decreased proton conductivity at high temperature, high manufacturing costs, and poor DMFC performance due to methanol crossover. Therefore, alternative PEMs must be developed to overcome the above drawbacks.

Radiation grafting has been a powerful technique for the development of alternative PEMs, in which grafts containing an ion-conducting group (electrolyte), such as sulfonic acid, are introduced into fluorinated polymer films, such as cross-linked polytetrafluoroethylene (cPTFE), poly(tetrafluoroethylene-*co*-hexafluoropropyrene) (FEP), poly(ethylene-*co*-tetrafluoroethylene) (ETFE), and poly(vinylidene fluoride) (PVDF), which act as hydrophobic matrices in PEMs.[2−8] This graft-type PEM has the advantages of resistance to methanol and low production costs. One of the graft-type PEMs is cross-linked cPTFE−PEM, which is prepared by radiation-induced grafting of styrene into a cPTFE substrate and subsequent sulfonation.[3,4,9,10] It has been shown that, as the degree of grafting (X_g) is varied from 7 to 75%, the ion exchange capacity (IEC) of the

Received: July 9, 2012
Revised: October 5, 2012
Published: November 6, 2012

cPTFE−PEM varies over a wide range up to 2.9 mol/g (Scheme 1). The cPTFE−PEM shows not only much higher

Scheme 1. Preparation Scheme of cPTFE−PEM

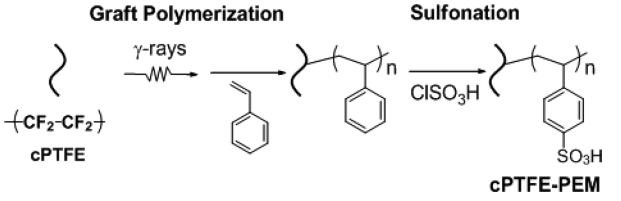

proton conductivity, but also lower methanol crossover, in comparison with perfluorinated PEMs.[4−7] Furthermore, in comparison with most aromatic-hydrocarbon-polymer-based PEMs, graft-type fluorinated PEMs, such as cPTFE−PEM, exhibit higher proton conductivity at lower grafting degrees and IECs.[11,12]

In the case of Nafion, its higher-order structure has been extensively investigated using scattering techniques.[13−19] An ionic cluster, which consists of water molecules surrounded by sulfonic acid groups acting as the interface between the water and the hydrophobic perfluorinated polymer backbone, has been proposed on the basis of the observations of the scattering maximum, the so-called "ionomer peak".[13] The formation of these clusters is thought to be the origin of ionic conductivity. Therefore, it is important to characterize the higher-order structure of the cPTFE−PEM to understand its outstanding properties. It should be noted that the higher-order structures of grafted PEMs can be analyzed in detail by comparing them with the structures obtained for the precursor cPTFE and polystyrene-grafted cPTFE films, because the grafted PEMs are well-known to maintain to some extend the crystalline structures of precursor original cPTFE and polystyrene grafted films. Thus, the higher-order structure of the cPTFE−PEM was investigated by SANS in comparison with the precursor films, a cPTFE polymer substrate and polystyrene-grafted cPTFE in the swollen state.

So far, the hierarchical structure of the cPTFE−PEM at the nano-to-meso scales, which will elucidate its unique properties (high ionic conductivity with a low IEC and lower methanol and water transmittance), was not resolved. In the present study, wide-Q measurements of small-angle scattering (SAS), including focusing SANS (FSANS), SANS, and small-angle X-ray scattering (SAXS), were carried out to obtain structural information on cPTFE−PEMs with various grafting degrees (X_g) up to 36% over a wide length scale from nanometer to micrometer. Because the hierarchical structure of cPTFE−PEMs was successfully revealed in the dried state, the relationship between the hierarchical structure and the above unique properties, such as the ionic conductivity and methanol and water transmittance of the cPTFE−PEM, is discussed.

EXPERIMENTAL SECTION

Materials and Sample Preparations. cPTFE−PEMs were prepared using both radiation-induced cross-linking and graft polymerization of styrene. Since they have been described in earlier publications,[3] the procedure for this present study is briefly outlined below. A cPTFE substrate (thickness of 50 μm) was parched for Hitachi Densen Co. Japan. The cPTFE film was preirradiated under argon atmosphere using γ-rays with a dose rate of 15 kGy/h form ^{60}Co source in Japan Atomic Energy Agency (JAEA) at Takasaki, Japan. The degree of grafting (X_g) of the cPTFE-*graft*-polystyrene was gravimetrically calculated using the following equation:

$$X_g = \frac{W_g - W_0}{W_0} \times 100 \quad (1)$$

where W_g and W_0 represent the weights of grafted and original cPTFE membranes, respectively. The nine sheets of grafted membranes (cPTFE-*graft*-PS) with X_g ranging from 0 to 36% were prepared. The grafted membranes were subsequently sulfonated in a 0.2 M chlorosulfonic acid solution of 1,2-dichloroethane at 60 °C for 6 h. Finally, the PTFE−PEM was washed in distilled water at 80 °C for 24 h.

Proton Conductivity. In-plane proton conductivity was determined by impedance measurement of the cPTFE−PEMs using the LCR HiTESTER 3522−50 (HIOKI E. E. CORPORATION, Japan) at 25 °C. The swollen cPTFE−PEM was sandwiched between two platinum-plate electrodes after wiping off excess water on the membrane surface. The proton conductivity σ (S/cm) was estimated from the obtained impedance, R (W) using the following equation

$$\sigma = \frac{w}{Rdl} \quad (2)$$

where w (cm) is the distance between the two electrodes, d (cm) is the membrane thickness, and l (cm) is the length of the membrane along the electrode. Samples were hydrated in distilled water at 25 °C for over 12 h prior to measurement.

Small-Angle Neutron Scattering (SANS). SANS experiments were performed using the small-angle neutron scattering spectrometer (SANS-J-II) installed at JRR-3 in JAEA, Tokai, Japan.[20] Both pinhole SANS (PSANS) and focusing SANS (FSANS) were carried out in order to cover a wide Q-range, where Q is defined by $Q = (4\pi/\lambda)\sin(\theta/2)$ (λ and θ being the wavelength and the scattering angle, respectively). The incident wavelength was 0.65 nm (wavelength resolution of 13%). In the case of PSANS, a two-dimensional ^{3}He position-sensitive detector collected the scattered neutrons from samples, and the sample-to-detector distances were 2.5 and 10.2 m. The size of source (A_0) and sample (A_s) aperture ware A_0 = 20 mm and A_s = 8 mm, respectively. Then, the covered Q-range for PSANS is $Q = 4 \times 10^{-2}$ to 1.2 nm^{-1}. On the other hand, FSANS experiments were performed with using 70 biconcave MgF_2 lenses and a high-resolution scintillation detector consisting of a position-sensitive photomultiplier (diameter of 5 in. and spatial resolution of 0.5 mm) coupled with ZnS/^{6}LiF scintillator (thickness of 0.2 mm), with A_0 = 3 mm and A_s = 16 mm, respectively. The sample-to-detector distance for FSANS was fixed at 9.4 m. The covered Q-range for FSANS was realized to $Q = 4 \times 10^{-3} - 5 \times 10^{-2}$ nm^{-1}. All measurements were performed at an ambient temperature (ca. 25 °C). After circular averaging, we subtracted for background scattering and converted the scattering intensity to the absolute intensity per sample volume by using a secondary standard of irradiated aluminum. Finally, the estimated incoherent scattering was subtracted from the absolute scattering intensity.

Small-Angle X-ray Scattering (SAXS). SAXS measurements were carried out using two SAXS spectrometers (NIMS-SAXS-II and NIMS-SAXS-III) at the National Institute of Materials Science (NIMS), Tsukuba, Japan,[21] in order to cover Q range from 7×10^{-2} to 13.5 nm^{-1}. The NIMS-SAXS-II consists of a two-dimensional confocal mirror to obtain high-flux Mo Kα beam with wavelength of 0.07 nm (NANO-Viewer, RIGAKU, Tokyo, Japan), a vacuum flight path, and multiwire two-dimensional position sensitive detector (2D-PSD) with an active area of 115 mm diameter (Hi-Star, Bruker Optik, GmbH, Germany), respectively. The sample-to-detector distance was 0.3 m, covering a Q-range of $7 \times 10^{-1} < Q < 13.5$ nm^{-1}. The NIMS-SAXS-III is Nano-STAR SAXS system (Bruker Optik, GmbH, Germany) using a Cr Kα beam with wavelength of 0.22 nm, which has a Göbel mirror and a 2D-PSD. The sample-to-detector distance was 1 m, covering Q range of $7 \times 10^{-2} < Q < 1.5$ nm^{-1}. The SAXS profiles were circularly averaged, and then were corrected for the absorption of the sample, instrumental background. The absolute

dx.doi.org/10.1021/ma301415r | Macromolecules 2012, 45, 9121−9127

SAXS intensity was obtained by using a secondary standard of glassy carbon with thickness of 1 mm.[21,22]

RESULTS

1. Proton Conductivity. Figure 1 shows the in-plane proton conductivity of the swollen cPTFE−PEM equilibrated

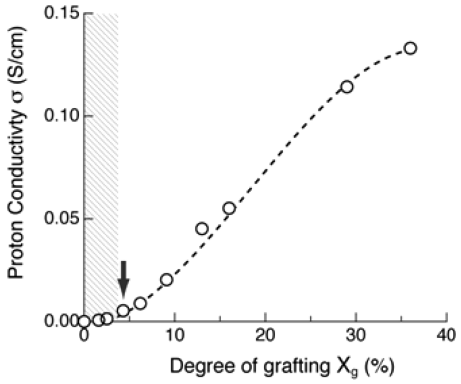

Figure 1. Degree of grafting (X_g) dependence of in-plane proton conductivity σ (S/cm) of the cPTFE−PEM at 25 °C in fully hydrated states.

in deionized water at 25 °C as a function of the X_g from 0% to 36%. The cPTFE−PEMs with X_g > 4.3% (down arrow shown in Figure 1) exhibited discernible proton conductivity. For X_g ranging from 4.3% to 36%, the proton conductivity systematically increased from 5.2 × 10^{-3} to 0.133 S/cm with increasing X_g. The X_g dependence of the proton conductivity is in good agreement with previously reported data.[3,7] The cPTFE−PEM with X_g = 15%, which shows a similar conductivity to that of Nafion, exhibits water uptake of 19%, which is slightly lower than that of Nafion. Even for cPTFE−PEM with X_g = 36%, the water uptake is 50%.

2. Characterization of the Hierarchical Structure of cPTFE−PEM. Figures 2 and 3 show the SANS (both FSANS and PSANS) and the SAXS profiles of dried cPTFE−PEMs with X_g ranging from 0% to 36% in the Q-ranges from 4 × 10^{-3} to 1.2 nm^{-1} and from 7 × 10^{-2} to 13 nm^{-1}, respectively. The combination of FSANS, SANS, and SAXS measurements enables the determination of the hierarchical structures of

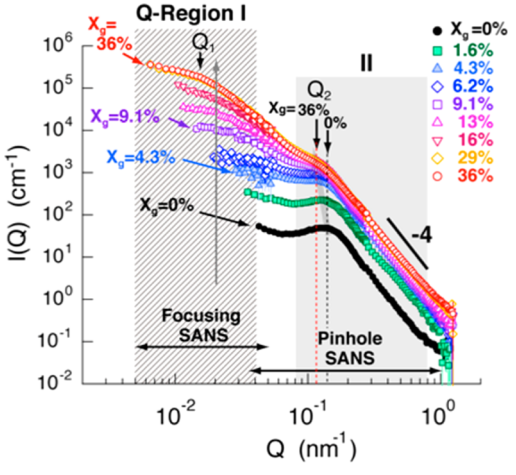

Figure 2. Variation of SANS profiles for cPTFE−PEM under dry states depending on the degree of grafting (X_g) from 0 to 36%.

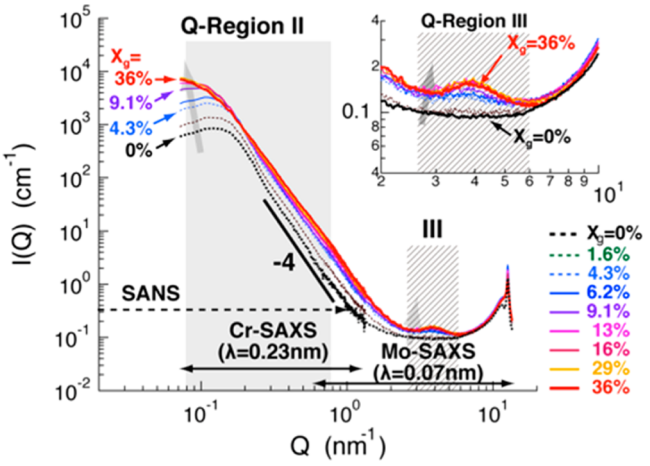

Figure 3. Variation of SAXS profiles for cPTFE−PEM under dry states depending on the degree of grafting (X_g) from 0 to 36%. The same cPTFE−PEM used for the SANS was used concurrently. Inset shows the expanded SAXS profiles in around Q-region III (Q = 2.0−10 nm^{-1}).

cPTFE−PEMs over a wide range from 0.5 nm to 1.6 μm in real d space. With increasing X_g of the membranes, changes in the SANS and SAXS profiles (Q positions of the peaks/shoulders and intensities) were observed. According to typical profiles and the dependency of the scattering intensity on X_g, to enable the detailed discussion of the hierarchical structures of the cPTFE−PEM, the scattering profiles were classified into three Q regions: Q-region I: 5 × 10^{-3} nm^{-1} < Q < 3 × 10^{-2} nm^{-1} (210 nm < d < 1.3 μm), Q-region II: 8 × 10^{-2} nm^{-1} < Q < 8 × 10^{-1} nm^{-1} (8.0 nm < d < 80 nm), and Q-region III: 2.5 nm^{-1} < Q < 6.0 nm^{-1} (1.0 nm < d < 2.5 nm).

2.1. Region I (SANS). In Q-region I (Q < 3 × 10^{-2} nm^{-1}; d > 210 nm), the SANS profiles were obtained by FSANS, and the change in the scattering profile is clearly observed with increasing X_g. The SANS intensity ($I(Q_1)$) at Q = 2 × 10^{-2} nm^{-1} was plotted as a function of X_g in Figure 4. The $I(Q_1)$ of

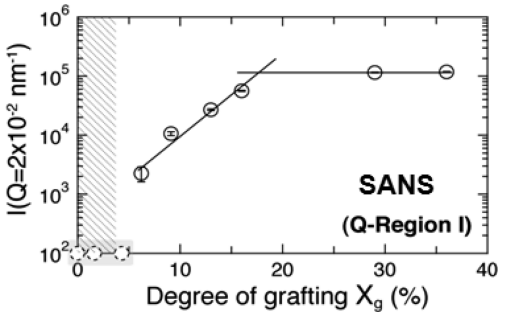

Figure 4. X_g dependence of the SANS intensity at Q_1 = 2 × 10^{-2} nm^{-1}, indicated by arrow on the SANS shown in Figure 2. For 0% < X_g < 1.6%, the SANS intensities could not be estimated, because the background-scattering is larger than those from the cPTFE−PEM.

the cPTFE−PEMs with 0% < X_g < 1.6% could not be determined from the SANS profile because of large background scattering. On the other hand, for the cPTFE−PEMs with 6.2% < X_g < 29%, the SANS intensity increased drastically, whereas the SANS intensity was nearly constant when X_g ranged between 29% and 36%. The increase of SANS intensity is due to the introduction of graft polymers, resulting in an increase in the scattering contrast.

dx.doi.org/10.1021/ma301415r | Macromolecules 2012, 45, 9121−9127

2.2. Region II (SANS/SAXS). In the Q-range from 8.0×10^{-2} to 8.0×10^{-1} nm^{-1} (8.0 nm < d < 80 nm), the SANS profiles of the cPTFE−PEMs exhibited a broad peak profile at around $Q = 1.3 \times 10^{-1}$ nm^{-1} (48 nm < d < 57 nm), which was similar in size to the lamellar d-spacing in the cPTFE substrate (X_g = 0%).[21] As shown in Figure 2, the SANS profile seemed to have a peak-like shape for the membranes with X_g < 9.1% and a shoulder-like shape for the membranes with X_g > 13%. In the Q-range from 3.0×10^{-1} to 1.0 nm^{-1}, the SANS profiles in the cPTFE substrate (X_g = 0%) obeyed Porod's law ($I(Q) \sim Q^{-4}$), originating in sharp interface between the amorphous and crystalline domains. The SANS profiles of the cPTFE−PEMs also exhibited Q^{-4} behavior, indicating a clear phase separation of the graft chains from the amorphous and crystalline domains in the cPTFE substrate.

As shown in Figure 3, the SAXS profiles of the dried cPTFE−PEMs showed similar profiles with a peak-like shape for the PEMs with X_g < 9.1% and a shoulder-like shape for the PEMs with X_g > 13%. The peak position (Q_2) and peak intensity ($I(Q_2)$) were plotted as a function of X_g, as shown in Figure 5 (a detailed discussion is provided below). The Q range that was higher than the peak position (0.3 nm^{-1} < Q < 1.0 nm^{-1}) also obeyed Porod's law.

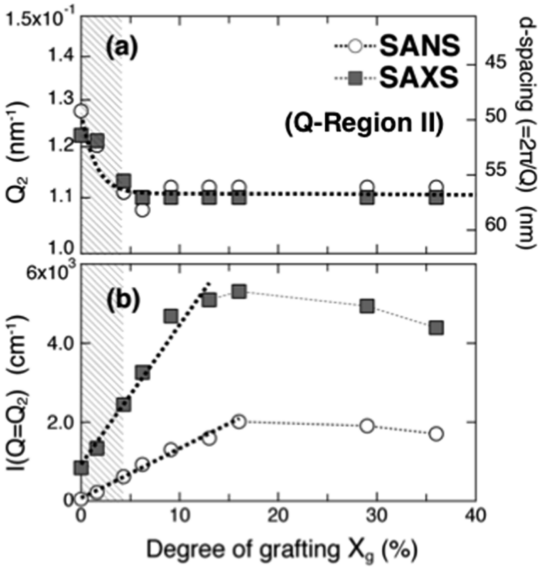

Figure 5. X_g dependences of (a) the peak-positions Q_2 and (b) the peak-intensity $I(Q_2)$, which are observed in (○) SANS and (■) SAXS in Q-region II (8×10^{-2} nm^{-1} < Q < 2×10^{-1} nm^{-1}).

2.3. Region III (SAXS). Because the SAXS measurements covered the higher Q-range up to 13 nm^{-1}, Q-region III (2.5 nm^{-1} < Q < 6.0 nm^{-1}, 1.0 nm < d < 2.5 nm) could be observed. In Q-region III, the SAXS profile of the cPTFE−PEMs with X_g > 4.3% exhibited a scattering maximum at approximately 3.7 nm^{-1}, which corresponded to ca. 1.7 nm. Figure 6 shows the intensity of the scattering maximum $I(Q_3)$ and the Q_3 position as a function of X_g. According to our previous study, this scattering maximum has not been observed in polyether ether ketone (PEEK) grafted only with polystyrene, which do not possess sulfo groups in the grafting layers. Furthermore, the peak profile was observed in a PEEK-based PEM prepared by radiation grafting.[23] Thus, it was concluded that the new scattering peaks should correspond to a medium-range order correlation distance between the sulfonic acid groups of the

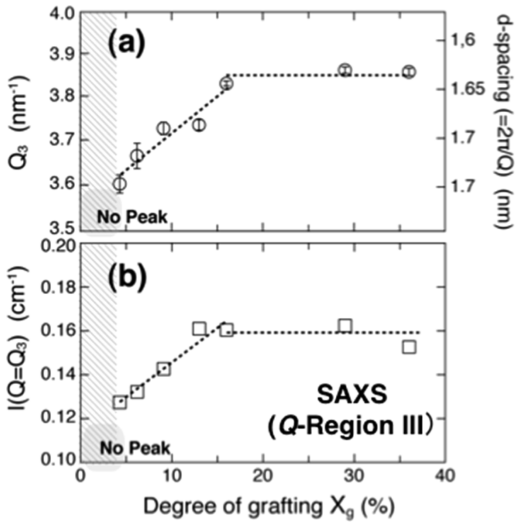

Figure 6. X_g dependences of (a) peak-positions (Q_3) and (b) peak-intensity ($I(Q_3)$) which are observed in SAXS around Q = 3.7 nm^{-1} (Q-region III).

graft polymers in the conducting layers of the cPTFE−PEM. It should be noted that these nano-order correlation distances of the sulfonic acid groups, which should act as ion channels, cannot be observed in Nafion.

■ DISCUSSION

1. Variation of the Hierarchical Structure of cPTFE−PEM During the Grafting Process. Wide-Q observations obtained through a combination of FSANS, PSANS, and SAXS analyses allowed for the systematic elucidation of the hierarchical structure in the cPTFE−PEM over an extremely wide length scale ranging from 0.6 nm to 1.6 μm (approximately 4 orders of magnitude in the length scale). As described in the Results, the cPTFE−PEM consists of three characteristic structures based on the dependency of the scattering intensity on X_g. In this section, the effect of the amount of ion-conducting layers consisting of grafted (polystyrenesulfonic acid), namely the value of X_g, on the hierarchical structure of the cPTFE−PEM is considered. The gradual change in the hierarchical structure of the PEMs at each grafting degree (X_g = 0, 4.3, 16, and 36%) is schematically illustrated in Figure 7.

$$0\% < X_g < 5\%$$

Although there was no significant change in the scattering profiles in Q-regions I and III (see Figures 2 and 3), the profiles in Q-region II (8×10^{-2} nm^{-1} < Q < 2×10^{-1} nm^{-1}) showed a gradual change in both the SANS and SAXS measurements. As shown in Figure 5, with an increase in X_g up to 4.3%, Q_2 shifted slightly toward a lower Q-value (from 48 to 57 nm in d spacing) with a linear increase in $I(Q_2)$. Accordingly, at a low degree of grafting (X_g < 5%), graft polymerization should be affected by the lamellar stacks in the cPTFE substrate with a lamellar spacing ($d_2 = 2\pi/Q_2$) of 48.3 nm, because they are in the same Q range as Q-region II (see Figure 7a).

With increasing X_g, the peak intensity ($I(Q_2)$) in both the SANS and SAXS profiles increased linearly but with different slopes for $I(Q_2)$ vs X_g. Namely, $I(Q_2)$ was strongly dependent on the radiation source (neutron/X-ray). The increase in the $I(Q_2)$ is due to increasing the scattering contrast ($\Delta\rho$). In the

dx.doi.org/10.1021/ma301415r | Macromolecules 2012, 45, 9121−9127

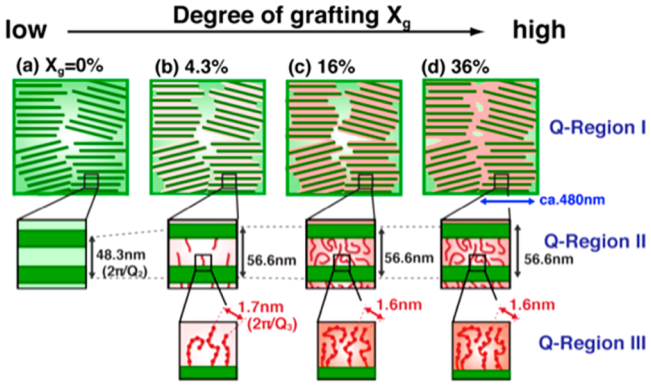

Figure 7. Schematic illustrations of the morphology change in the hierarchical structure for cPTFE–PEM under dry states with increasing the degree of grafting, which are drawn from the analysis in a wide-Q range of SAS. (a) X_g = 0% (before grafting), (b) 4.3%, (c) 29%, and (d) 36%. The illustrations show the mechanism of the graft polymerization of cPTFE–PEM.

original cPTFE film (X_g = 0), $\Delta\rho$ corresponds to the difference between the scattering length density of the crystalline (ρ_c) and amorphous (ρ_a) regions ($\Delta\rho = \rho_c - \rho_a$). During the initial stages of the graft polymerization process, the observed changes in $\Delta\rho$ reflect the change in ρ_a, because the change in ρ_c is negligibly small. Thus, the increase of $I(Q_2)$ was influenced mainly by the change in $\Delta\rho$ at X_g < 5%. On the other hand, the different slopes for $I(Q_2)$ is due to the difference in $\Delta\rho$ values between X-rays and neutrons. The $\Delta\rho$ between graft polymer chains and the crystalline region of a cPTFE for X-rays is larger than that for neutrons. Furthermore, the SANS and SAXS profiles in the Q-range that was higher than the peak position (Q_2) maintained a Q^{-4} behavior with increasing X_g. These observations suggest that the graft polymerization proceeded in the amorphous phase between the lamellar crystals of the cPTFE during the initial stages, resulting in the formation of clearly phase-separated conducting layers consisting of graft polymers, which were segregated from the amorphous and crystalline domains in the cPTFE substrate, as illustrated in Figure 7b.

$5\% < X_g < 15\%$

In Q-region II, as shown in Figure 5, $I(Q_2)$ constantly increased, whereas the peak position of Q_2 remained at a constant value of 0.11 nm^{-1} (d = 57 nm). This result indicates that the graft polymerization proceeded continuously in the amorphous phase in the lamellar stacks of the cPTFE and likely maintained the lamellar spacing as a result of crystalline lattice restriction. The only possible explanation for why only the intensity at Q_2 increased is that the graft polymerization continued inside, as well as outside, of the lamellar stacks, such that the thin layers of graft polymers covered the surfaces of the crystallites in the cPTFE substrates.

In Q-region I, the scattering intensity at $Q_1 = 2 \times 10^{-2}$ nm^{-1} (d = 314 nm) was imperceptible in the PEMs with X_g lower than 4.3%; however, the intensity in this region gradually increased in the PEMs with X_g > 6.2%, as shown in Figure 4. The linear increase in the scattering intensities in Q-region I with the d spacing ranging from 210 nm to 1.3 μm indicates that the size of the newly generated graft domains increased gradually and reached more than a micrometer in length. The PEM with the highest X_g (36%) showed the crossover point of Q (Q_1) and deviated from the asymptotic power-law behavior, with $Q = 1.3 \times 10^{-2}$ nm^{-1} (d = 480 nm). This Q_1 is nearly equal to the crossover point in the profile of the cPTFE substrate ($Q = 1.2 \times 10^{-2}$ nm^{-1}). On the basis of the above observations, a fitting analysis of the SANS profile of the cPTFE substrate was conducted with a stacked lamellar model. This analysis showed that the average lamellar spacing and crystalline thickness were 37.7 and 11.4 nm, respectively, and that the crystallite diameter and length was 430 nm. No structural information between 430 nm and 1.6 μm indicate that the crystallite length might be out of the Q range (d > 1.6 μm) in a cPTFE substrate. Namely, the conducting layers (graft domains) covering the surfaces of the crystallites of the cPTFE substrate were estimated to be approximately 430 nm (diameter) and beyond the Q range of this measurement (length). The size of an ion cluster in Nafion is approximately 3–5 nm,[13–19] and thus, it should be emphasized that the ion channels in the cPTFE–PEM possess a structure totally different from that in Nafion. The graft polymers propagated not only inside but also outside of the lamellar stacks, resulting in the expansion of the conducting layers covering the crystallites (top of Figure 7c), because graft polymerization between the lamellar crystals was suppressed, as suggested in Q-region II.

In Q-region III, a new peak appeared at approximately Q = 3.7 nm^{-1}, which should be attributed to the length of the sulfonic acid groups of the graft polymers (vide ante) in the PEM with X_g > 6.3%. Namely, there is a nanoscale internal structure in the conducting layers in the cPTFE–PEM that has not been reported in Nafion. As shown in Figure 6, both the peak position (Q_3) and intensity ($I(Q_3)$) increased linearly with increasing X_g, indicating that the graft polymers built up an apparent internal structure with a characteristic length of approximately 1.7–1.9 nm (medium-range order correlation), probably due to the repulsive ionic interaction between sulfonic acid groups in the graft polymers, and the intermolecular distance decreased because of an increase in the number of sulfonic acid groups with increasing X_g from 4.3% to 16%. Note that in the PEMs with X_g < 4.3%, the correlation between the sulfonic acid groups was barely detected because they were distributed sparsely in the grafting regions.

$X_g > 15\%$

Even though the proton conductivity of the cPTFE–PEM continuously increased with increasing X_g above 15%, the peak positions and their intensities in the Q-regions I–III did not show clear changes.

In Q-region I, the scattering intensity at $Q = 2 \times 10^{-2}$ nm^{-1} (d = 310 nm) was constant in the PEMs with X_g > 15%. Because the length of the grafting layers on the surfaces of the crystallite is greater than ca. 1.6 μm, which corresponds to the observable maximum length in the present observations, a change in the scattering profiles could be observed, even with an increase in X_g from 15% to 36%. As previously described, Q_1 in the cPTFE substrate is attributed to the diameter of the crystallite in the cPTFE substrate. The degree of crystallinity of the cPTFE substrate was reported to be 30–40% based on previous differential scanning calorimetry and wide-angle X-ray diffraction measurements.[11] Each crystallite seemed to be adjoining in the cPTFE substrate. Accordingly, as shown in Figure 7(d), the grafting layers were phase-separated from the cPTFE substrate, and thus cover the 480-nm-diameter crystallites (the length of the crystallites is above the observed

dx.doi.org/10.1021/ma301415r | Macromolecules 2012, 45, 9121–9127

Q region (>1.6 μm)). The graft domains around the crystallites are connected with the adjoining domains; accordingly, the PEM at higher degrees of grafting has conductivity higher than that of Nafion. It should be noted that the ion-channel structures of the cPTFE−PEM, which consist of the graft polymers, were strongly affected by the crystallite and lamellar structures in the cPTFE substrate.

Contrary to the constant value of $I(Q_1)$ in Q-region I, the $I(Q_2)$ in Q-region II slightly decreased with an increase in X_g from 15% to 36% in both the SANS and SAXS profiles (Figure 5). It has been reported that the crystallinity of polymer substrates remains constant at low degrees of grafting and then slightly decreases with increasing X_g.[2,24] Actually, in the Q-range $10 < Q < 13$ nm^{-1} ($0.5 < d < 0.6$ nm) in the WAXS region, broad and sharp peak profiles were observed at $Q = 11.5$ and 12.8 nm^{-1}, reflecting the amorphous and crystalline components in the cPTFE substrate, respectively.[25] The $I(Q)$ of the SANS and SAXS profiles decreased with an increase in X_g from 15% to 36%; thus, the decreased crystallinity should be due to the destruction of the lamellar stacks near the interface with the grafting layers as a result of the graft polymerization. Because of the amount of repeating grafting layers located around the lamellar crystals, $I(Q_2)$ should decrease as a result of the destruction of the lamellar stacks in the cPTFE substrate. However, the repeating length of the lamellar stacks did not change in the cPTFE−PEM with $X_g > 15\%$, and the decreased value of $I(Q_2)$ is negligible. Furthermore, with increasing X_g from 0 to 36%, the degree of crystallinity decreased only from 39.6 to 39.0%, suggesting that the effect of the grafting on the degree of crystallinity is negligibly small. Thus, the destruction of the lamellar stacks in this X_g region occurred over a very limited area of the crystallites.

2. Relationship between the Hierarchical Structure and the Electrolyte Properties of cPTFE−PEM. On the basis of the results obtained from the wide-Q observations of cPTFE−PEMs with various X_g up to 36% using FSANS, SANS, and SAXS, the relationship between its hierarchical structure, which is composed of conducting layers (graft domains) in the lamellar stacks with 48−57 nm spacing on the surfaces of 480-nm-diameter crystallites and ultrasmall structures with 1.7 nm correlation distance between the sulfonic acid groups in the conducting layers, and electrolyte properties was considered. As shown in Figure 1, the cPTFE−PEMs with $X_g < 4.3\%$ exhibited proton conductivity, although at a minimum level (5.2×10^{-3} S/cm). However, when X_g just exceeded 5%, conductivity increased steeply with increasing X_g. Namely, the ion-conducting paths could be connected to each other, even with a lower IEC (0.6 mmol/g) compared with that in Nafion. Accordingly, the higher conductivity of the cPTFE−PEM compared with that of other aromatic-hydrocarbon-polymer-based PEMs with similar IECs can be explained by the fact that the ion channels, which consist of the graft polymers that exist locally in the amorphous layer in the lamellar stacks and around the crystallites, contain condensed ionic groups (sulfonic acid groups) that are favorable for high conductivity even at a low sulfonic acid concentration. With a grafting degree above 15%, the grafting layers were phase-separated from the cPTFE substrate and covered the 480-nm-diameter crystallites (the length of the crystallite is above the observed Q region (>1.6 μm)). Because the graft domains around the crystallites are connected with the adjoining domains, the PEM at higher grafting degrees has conductivity higher than that of Nafion.

Scattering profiles of Nafion exhibit two peaks around Q = 0.4 nm^{-1} and 1.5 nm^{-1}, respectively.[16−18] The peak in the low-Q region are attributed to the large crystalline domains of a lamellar structure in the matrix, which is similar to that of cPTFE−PEM observed in a scattering profile around $Q = 0.15$ nm^{-1}. However, recent scattering results of Nafion have no peak in the low-Q region[18] probably because this peak depends on the manufacturing process of Nafion membranes. In contrast, the peak in similar low-Q region in the cPTFE−PEM profile is distinct and its position is dependent on the degree of crystallinity of the cPTFE−PEM, which can be controlled by radiation doses. The peak of Nafion in the high-Q region (around $Q = 1.5$ nm^{-1}) are known as an "ionomer peak". The "ionomer peak" is mainly attributed to a water channel.[18] On the other hand, the peak profile of cPTFE−PEM in the Q-range of Q = 3.5−3.9 nm^{-1} is originated from the correlation distance between the sulfonic acid groups of the graft polymers in the conducting layers of the cPTFE−PEM. The origin of peaks is remarkably different from each other. Thus, the peak-position shifted to lower Q value for Nafion, whereas one shifted to higher Q values for cPTFE−PEM, with increasing proton conductivity.

As the previous work of other graft-type PEM, PVDF-*g*-PSSA was characterized using SAXS by Hietala et al.[8] PVDF-*g*-PSSA exhibited discernible proton conductivity at X_g = 30%. They carried out the measurement of the three kinds of PVDF-*g*-PSSA with X_g =23, 54, and 100%. The following two differences are prominent in X_g-dependence of hierarchical structure for cPTFE−PEM and PVDF-*g*-PSSA. (1) For PVDF-*g*-PSSA, the lamellar d-spacing is continuously increased with increasing the X_g, even up to X_g = 30% or higher, whereas for cPTFE−PEM the lamellar d-spacing increased only with the increase of X_g up to 5% and are constant in the X_g ranges higher than 5%. (2) The peak profile of the PVDF-*g*-PSSA at a high-Q region, which is similar to the ionomer peak of Nafion, is clearly different from that of the cPTFE−PEM.

The other unique property of the cPTFE−PEM is its very low permeability to small molecules such as methanol (so-called the "low methanol crossover" in DMFCs) in comparison with that Nafion.[3] The SAXS observation showed a nanoscale internal structure (1.7−1.9 nm) corresponding to a medium-range order correlation distance between the sulfonic acid groups of the graft polymers in the conducting layer. Recently, based on radiotracer permeation with tritium labeling, it has been reported that the self-diffusion coefficient of water in the cPTFE−PEM is lower than that in Nafion.[26] The lower water permeability likely originates from the same internal structures of the conducting layers. Namely, the nano-order network structure consisting of sulfonic acid groups located in a medium-range order correlation distance to each other should suppress the diffusion of water and methanol molecules in the channels, in comparison with that in Nafion.

Finally, the importance of the cross-linking structures in the cPTFE−PEM on the electrolyte and mechanical properties should be addressed. To date, it has been reported that the mechanical strength of a PTFE substrate is increased by radiation cross-linking under particular irradiation conditions[8,9] because the crystalline morphology, such as the size and shape of the crystallites and the lamellar stacks in the substrate, is affected by the absorption dose and dose rate in the radiation-induced cross-linking process. In this study, it was clearly shown that the size and shape of the crystallites and the lamellar stacks in the cPTFE substrate play a crucial role in the

dx.doi.org/10.1021/ma301415r | *Macromolecules* 2012, 45, 9121−9127

formation of the internal and external structures of the conducting layers, which consist of the graft polymers, in the cPTFE−PEM. Thus, the radiation-induced cross-linking process may be utilized to control not only the mechanical strength, but also the electrolyte properties, by changing the size and shape of the ion channels, which should lead to further improvement in the required properties of graft-type PEMs.

■ CONCLUSION

The hierarchical structure of cPTFE−PEM has been characterized as being composed of conducting layers (graft domains) in lamellar stacks with 48−57 nm spacing on the surfaces of 480 nm-diameter crystallites and ultrasmall structures with 1.7 nm correlation distance of the sulfonic acid groups in the conducting layers by the combination of FSANS, SANS, and SAXS in a wide-Q range from 5×10^{-3} to 13 nm^{-1}. According to typical scattering profiles and the dependency of the scattering intensity of the dried cPTFE−PEM on X_g, the scattering profiles were classified into three Q-regions. The PEM with grafting degrees less than 15% possessed only grafting layers in the amorphous layers of the lamellar stacks of cPTFE. An increase in the lamellar spacing of 20% with the increases of the grafting degree up to 5%, while the lamellar spacing remained constant with grafting degrees above 5% owing to the crystalline restriction. With grafting degrees of greater than 15%, the grafting domains were phase-separated from the cPTFE substrate and covered the crystallites with a diameter of 480 nm. The graft domains around the crystallites were connected with the adjoining domains; accordingly, the PEM with a higher grafting degree had conductivity higher than that of Nafion. The nano-order network structure consisting of sulfonic acid groups located in the conducting layers of cPTFE−PEM corresponded to medium-range order correlation distance to each other. The nano-order correlation distances of the sulfonic acid groups, which cannot be observed in Nafion, should result in methanol and water crossover levels lower than those in Nafion.

■ AUTHOR INFORMATION

Corresponding Author

*E-mail: (Y.M.) maekawa.yasunari@jaea.go.jp; (S.K.) skoizumi@mx.ibaraki.ac.jp.

Present Addresses

[⊥]Research Center for Neutron Science & Technology, Comprehensive Research Organization for Science and Society (CROSS), 162−1 Shirakata, Tokai, Ibaraki 319−1106, Japan.
[∥]College of Engineering, Ibaraki University, 4−12−1 Nakanarusawa, Hitachi, Ibaraki 316−8511, Japan.

Notes

The authors declare no competing financial interest.

■ ACKNOWLEDGMENTS

This work was supported by a Grant-in-Aid for Young Scientists (Grant No. 20760479) from the Ministry of Education, Culture, Sports, Science, and Technology, of Japan. This work was performed under the NIMS-RIKEN-JAEA Cooperative Research Program on Quantum Beam Science and Technology. The authors would like to thank Enago (www.enago.jp) for the English language review.

■ REFERENCES

(1) Mauritz, K. A.; Moore, R. B. *Chem. Rev.* **2004**, *104*, 4535−4585.
(2) Tamada, M.; Maekawa, Y. Radiation Processing of Polymers and Its Applications. In *Charged Particles and Photon Interactions with Matter*; Hatano, Y., Katsumura, Y., Mozumder, A. (Eds.), CRC Press: Boca Raton, FL, 2011; Chapter 27, pp 737−759.
(3) Yamaki, T.; Asano, M.; Maekawa, Y.; Morita, Y.; Suwa, T.; Chen, J.; Tsubokawa, N.; Kobayashi, K.; Kubota, H.; Yoshida, M. *Radiat. Phys. Chem.* **2003**, *67*, 403−407.
(4) Sato, R.; Ikeda, S.; Iida, M.; Oshima, A.; Tabata, Y.; Washio, M. *Nucl. Instrum. Meth. B* **2003**, *208*, 424−428.
(5) Gürsel, S. A.; Gubler, L.; Gupta, B.; Scherer., G. G. *Adv. Polym. Sci.* **2008**, *215*, 157−217.
(6) Schmidt, T. J.; Simbeck, K.; Scherer, G. G. *J. Electrochem. Soc.* **2005**, *152*, A93−A97.
(7) Chen, J.; Asano, M.; Yamaki, T.; Yoshida, M. *J. Power Sources* **2006**, *158*, 69−77.
(8) Hietala, S.; Holmberg, S.; Nasman, L.; Ostrovskii, D.; Paronen, M.; Serimaa, R.; Sundholm, F.; et al. *Angew Makromol Chem Makromol.* **1997**, *253*, 151−167.
(9) Sun, J.; Zhang, Y.; Zhong, X.; Zhu, X. *Radiat. Phys. Chem.* **1994**, *44*, 655−659.
(10) Oshima, A.; Tabata, Y.; Kudo, H.; Seguchi, T. *Radiat. Phys. Chem.* **1995**, *45*, 269−273.
(11) Chen, J.; Asano, M.; Maekawa, Y.; Yoshida, M. *J. Membr. Sci.* **2006**, *277*, 249−257.
(12) Rikukawa, M.; Sanui, K. *Prog. Polym. Sci.* **2000**, *25*, 1463−1502.
(13) Gierke, T. D.; Munn, G. E.; Wilson, F. C. *J. Polym. Sci., Polym. Phys. Ed.* **1981**, *19*, 1687−1704.
(14) Fujimura, M.; Hashimoto, T.; Kawai, H. *Macromolecules* **1982**, *15*, 136−144.
(15) Gebel, G. *Polymer* **2000**, *41*, 5829−5838.
(16) Rubatat, L.; Rollet, A. L.; Gebel, G.; Diat, O. *Macromolecules* **2002**, *35*, 4050−4055.
(17) Kim, M. -H.; Glinka, C. J.; Grot, S. A.; Grot, W. G. *Macromolecules* **2006**, *39*, 4775−4787.
(18) Schmidt-Rohr, K.; Chen, Q. *Nat. Mater.* **2008**, *7*, 75−83.
(19) Iwase, H.; Koizumi, S.; Iikura, H.; Matsubayashi, M.; Yamaguchi, D.; Maekawa, Y.; Hashimoto, T. *Nucl. Instrum. Methods A* **2009**, *65*, 95−98.
(20) Koizumi, S.; Iwase, H.; Suzuki, J.; Oku, T.; Motokawa, R.; Sasao, H.; Tanaka, H.; Yamaguchi, D.; Shimizu, H. M.; Hashimoto, T. *J. Appl. Crystallogr.* **2007**, *40*, s474−s479.
(21) Ohnuma, M.; Suzuki, J.; Ohtsuka, S.; Kim, S. W.; Kaito, T.; Inoue, M.; Kitazawa, H. *Acta Mater.* **2009**, *57*, 5571−5581.
(22) Zhang, F.; Ilavsky, J.; Long, G. G.; Quintana, J. P. G.; Allen, A. J.; Jemian, P. R. *Metall. Mater. Trans. A* **2010**, *41*, 1151−1158.
(23) Hasegawa, S.; Takahashi, S.; Iwase, H.; Koizumi, S.; Morishita, N.; Sato, K.; Narita, T.; Ohnuma, M.; Maekawa, Y. *Polymer* **2011**, *52*, 98−106.
(24) Chapiro, A., In *Radiation Chemistry of Polymeric System*, Interscience Publishers, John Wiley & Sons: New York, 1962; Chapter XII.
(25) Ścigała, R.; Wlochowicz, A. *Acta Polym.* **1989**, *40*, 15−19.
(26) Sawada, S.; Yamaki, T.; Nishimura, H.; Asano, M.; Suzuki, A.; Terai, T.; Maekawa, Y. *Solid State Ionics* **2008**, *179*, 1611−1614.